Quantum Inf Process (2015) 14:3317–3333
DOI 10.1007/s11128-015-1039-4

Entanglement of four-qubit rank-2 mixed states

Eylee Jung[1] · **DaeKil Park**[1,2]

Received: 5 February 2015 / Accepted: 22 May 2015 / Published online: 11 June 2015

Abstract It is known that there are three maximally entangled states $|\Phi_1\rangle = (|0000\rangle + |1111\rangle)/\sqrt{2}$, $|\Phi_2\rangle = (\sqrt{2}|1111\rangle + |1000\rangle + |0100\rangle + |0010\rangle + |0001\rangle)/\sqrt{6}$, and $|\Phi_3\rangle = (|1111\rangle + |1100\rangle + |0010\rangle + |0001\rangle)/2$ in four-qubit system. It is also known that there are three independent measures $\mathcal{F}_j^{(4)}$ $(j = 1, 2, 3)$ for true four-way quantum entanglement in the same system. In this paper, we compute $\mathcal{F}_j^{(4)}$ and their corresponding linear monotones $\mathcal{G}_j^{(4)}$ for three rank-two mixed states $\rho_j = p|\Phi_j\rangle\langle\Phi_j| + (1-p)|W_4\rangle\langle W_4|$, where $|W_4\rangle = (|0111\rangle + |1011\rangle + |1101\rangle + |1110\rangle)/2$. We discuss the possible applications of our results briefly.

Keywords Entanglement · SLOCC-Classification · Four-qubit mixed states

1 Introduction

Recently, much attention is being paid to quantum information theory (QIT) and quantum technology (QT) [1]. Most important notion in QIT and QT is a quantum correlation, which is usually termed by entanglement [2] of given quantum states. As shown for last two decades, it plays a central role in quantum teleportation [3], superdense coding [4], quantum cloning [5], and quantum cryptography [6,7]. It is also quantum entanglement, which makes the quantum computer[1] outperform the

[1] The current status of quantum computer technology was reviewed in Ref. [8].

✉ DaeKil Park
dkpark@kyungnam.ac.kr

[1] Department of Electronic Engineering, Kyungnam University, Changwon 631-701, Korea

[2] Department of Physics, Kyungnam University, Changwon 631-701, Korea

classical one [9]. Thus, it is very important to understand how to quantify and how to characterize the entanglement.

1.1 Entanglement measures

For bipartite quantum system, many entanglement measures were constructed before such as distillable entanglement [10], entanglement of formation (EOF) [10], and relative entropy of entanglement (REE) [11,12].

The distillable entanglement is defined to quantify how many maximally entangled states can be constructed from the copies of the given quantum state in the asymptotic region. Thus, in order to compute the distillable entanglement, we should find the optimal purification (or distillation) protocol. If, for example, the optimal protocol generates n maximally entangled states from m copies of the quantum state ρ, the distillation entanglement for ρ is given by

$$D(\rho) = \lim_{m\to\infty} \frac{n}{m}. \tag{1.1}$$

Although the distillable entanglement is well-defined, its analytical calculation is very difficult because it is highly nontrivial task to find the optimal purification protocol except very rare cases [13–16].

REE of a given quantum state ρ is defined as

$$E_R(\rho) = \min_{\sigma\in\mathcal{D}} S(\rho||\sigma), \tag{1.2}$$

where $\mathcal{D}$ is a set of separable states and $S(\rho||\sigma)$ is a quantum relative entropy, that is $S(\rho||\sigma) = \mathrm{tr}(\rho\ln\rho - \rho\ln\sigma)$. It is known that $E_R(\rho)$ is an upper bound of the distillable entanglement. However, for REE, it is also highly nontrivial task to find the closest separable state σ of the given quantum state ρ. Still, therefore, we do not know how to compute REE analytically even in the two-qubit system except rare cases [17–22].

The EOF for bipartite pure states is defined as a von Neumann entropy of each party, which is derived by tracing out other party. For mixed state, it is defined via a convex-roof method [10,23];

$$E_F(\rho) = \min \sum_j p_j E_F(\psi_j), \tag{1.3}$$

where minimum is taken over all possible pure-state decompositions, i.e., $\rho = \sum_j p_j|\psi_j\rangle\langle\psi_j|$, with $0 \le p_j \le 1$. The decomposition which minimizes $\sum_j p_j E_F(\psi_j)$ is called the optimal decomposition. For two-qubit system, EOF is expressed as [24,25]

$$E_F(C) = h\left(\frac{1+\sqrt{1-C^2}}{2}\right), \tag{1.4}$$

where $h(x)$ is a binary entropy function $h(x) = -x \ln x - (1-x)\ln(1-x)$, and C is called the concurrence. For two-qubit pure state $|\psi\rangle = \psi_{ij}|ij\rangle$ with $(i, j = 0, 1)$, C is given by

$$C = |\epsilon_{i_1 i_2}\epsilon_{j_1 j_2}\psi_{i_1 j_1}\psi_{i_2 j_2}| = 2|\psi_{00}\psi_{11} - \psi_{01}\psi_{10}|, \tag{1.5}$$

where the Einstein convention is understood, and $\epsilon_{\mu\nu}$ is an antisymmetric tensor. For two-qubit mixed state ρ, the concurrence $C(\rho)$ can be computed by $C = \max(\lambda_1 - \lambda_2 - \lambda_3 - \lambda_4, 0)$, where $\{\lambda_1^2, \lambda_2^2, \lambda_3^2, \lambda_4^2\}$ are eigenvalues of $\rho(\sigma_y \otimes \sigma_y)\rho^*(\sigma_y \otimes \sigma_y)$ with decreasing order. Thus, one can compute the EOF for all two-qubit states in principle.

1.2 Classification of entanglement

Although quantification of the entanglement is important, it is equally important to classify the entanglement, i.e., to classify the quantum states into the different types of entanglement. The most popular classification scheme is a classification through a stochastic local operation and classical communication (SLOCC) [26]. If $|\psi\rangle$ and $|\Phi\rangle$ are in same SLOCC class, this means that $|\psi\rangle$ and $|\phi\rangle$ can be used to implement same task of quantum information process although the probability of success for this task is different. Mathematically, if two n-party states $|\psi\rangle$ and $|\phi\rangle$ are in the same SLOCC class, they are related to each other by $|\psi\rangle = A_1 \otimes A_2 \otimes \cdots \otimes A_n|\phi\rangle$ with $\{A_j\}$ being arbitrary invertible local operators.[2] Moreover, it is more useful to restrict ourselves to SLOCC transformation where all $\{A_j\}$ belong to SL(2, C), the group of 2×2 complex matrices having determinant equal to 1. In the three-qubit pure-state system, it was shown [27] that there are six different SLOCC classes, fully separable, three bi-separable, W, and Greenberger–Horne–Zeilinger (GHZ) classes. Subsequently, the classification was extended to the three-qubit mixed-state system [28].

The SLOCC transformation enables us to construct the entanglement measures for the multipartite states. As Ref. [29] showed, any linearly homogeneous positive function of a pure state that is invariant under determinant 1 SLOCC operations is an entanglement monotone. One can show that the concurrence C in Eq. (1.5) is such an entanglement monotone as follows. Let $|\psi\rangle = \psi_{ij}|ij\rangle$ with $i, j = 0, 1$. Then, $|\tilde{\psi}\rangle \equiv (A \otimes B)|\psi\rangle = \tilde{\psi}_{ij}|ij\rangle$, where $\tilde{\psi}_{ij} = \psi_{\alpha\beta}A_{i\alpha}B_{j\beta}$. Using $\epsilon_{ij}M_{i\alpha}M_{j\beta} = (\det M)\epsilon_{\alpha\beta}$ for arbitrary matrix M, it is easy to show $\epsilon_{i_1 i_2}\epsilon_{j_1 j_2}\tilde{\psi}_{i_1 j_1}\tilde{\psi}_{i_2 j_2} = (\det A)(\det B)\epsilon_{i_1 i_2}\epsilon_{j_1 j_2}\psi_{i_1 j_1}\psi_{i_2 j_2}$, which implies that C is invariant under determinant 1 SLOCC operations.

The theorem in Ref. [29], i.e., *a linearly homogeneous positive function that remains invariant under determinant* 1 *SLOCC operation is an entanglement monotone*, can be applied to the three-qubit system. If $|\psi\rangle = \psi_{ijk}|ijk\rangle$, the invariant monotone is

$$\tau_3 = \left|2\epsilon_{i_1 i_2}\epsilon_{i_3 i_4}\epsilon_{j_1 j_2}\epsilon_{j_3 j_4}\epsilon_{k_1 k_3}\epsilon_{k_2 k_4}\psi_{i_1 j_1 k_1}\psi_{i_2 j_2 k_2}\psi_{i_3 j_3 k_3}\psi_{i_4 j_4 k_4}\right|^{1/2}. \tag{1.6}$$

[2] For complete proof on the connection between SLOCC and local operations, see Appendix A of Ref. [27].

This is exactly the same with a square root of the residual entanglement[3] introduced in Ref. [30]. The three-tangle (1.6) has following properties. If $|\psi\rangle$ is a fully separable or a partially separable state, its three-tangle completely vanishes. Thus, τ_3 measures the true three-way entanglement. It also gives $\tau_3(\mathrm{GHZ}_3) = 1$ and $\tau_3(W_3) = 0$ to the three-way entangled states, where

$$|\mathrm{GHZ}_3\rangle \frac{1}{\sqrt{2}}(|000\rangle + |111\rangle) \quad |W_3\rangle = \frac{1}{\sqrt{3}}(|001\rangle + |010\rangle + |100\rangle). \tag{1.7}$$

For mixed state, quantification of the entanglement is usually defined via a convex-roof method [10,23]. Although the concurrence for an arbitrary two-qubit mixed state can be, in principle, computed following the procedure introduced in Ref. [24,25], still we do not know how to compute the three-tangle (or residual entanglement) for an arbitrary three-qubit mixed state. However, the residual entanglement for several special mixtures was computed in Ref. [31–35]. More recently, the three-tangle for all GHZ-symmetric states [36] was computed analytically [37].

It is also possible to construct the SLOCC-invariant monotones in the higher-qubit systems. In the higher-qubit systems, however, there are many independent monotones, because the number of independent SLOCC-invariant monotones is equal to the degrees of freedom of pure quantum state minus the degrees of freedom induced by the determinant 1 SLOCC operations. For example, there are $2(2^n-1)-6n$ independent monotones in n-qubit system. Thus, in four-qubit system, there are six invariant monotones. Among them, it was shown in Ref. [38–40] by making use of the antilinearity [23] that there are following three independent monotones which measure the true four-way entanglement:

$$\begin{aligned}
\mathcal{F}_1^{(4)} &= (\sigma_\mu\sigma_\nu\sigma_2\sigma_2) \bullet (\sigma^\mu\sigma_2\sigma_\lambda\sigma_2) \bullet (\sigma_2\sigma^\nu\sigma^\lambda\sigma_2) \\
\mathcal{F}_2^{(4)} &= (\sigma_\mu\sigma_\nu\sigma_2\sigma_2) \bullet (\sigma^\mu\sigma_2\sigma_\lambda\sigma_2) \bullet (\sigma_2\sigma^\nu\sigma_2\sigma_\tau) \bullet (\sigma_2\sigma_2\sigma^\lambda\sigma^\tau) \\
\mathcal{F}_3^{(4)} &= \frac{1}{2}(\sigma_\mu\sigma_\nu\sigma_2\sigma_2) \bullet (\sigma^\mu\sigma^\nu\sigma_2\sigma_2) \bullet (\sigma_\rho\sigma_2\sigma_\tau\sigma_2) \bullet (\sigma^\rho\sigma_2\sigma^\tau\sigma_2) \\
&\quad \bullet(\sigma_\kappa\sigma_2\sigma_2\sigma_\lambda) \bullet (\sigma^\kappa\sigma_2\sigma_2\sigma^\lambda),
\end{aligned} \tag{1.8}$$

where $\sigma_1 = \mathbb{1}_2, \sigma_1 = \sigma_x, \sigma_2 = \sigma_y, \sigma_3 = \sigma_z$, and the Einstein convention is introduced with a metric $g^{\mu\nu} = \mathrm{diag}\{-1, 1, 0, 1\}$. Furthermore, it was shown in Ref. [41] that there are following three maximally entangled states in four-qubit system:

$$\begin{aligned}
|\Phi_1\rangle &= \frac{1}{\sqrt{2}}\big(|0000\rangle + |1111\rangle\big) \\
|\Phi_2\rangle &= \frac{1}{\sqrt{6}}\Big(\sqrt{2}|1111\rangle + |1000\rangle + |0100\rangle + |0010\rangle + |0001\rangle\Big) \\
|\Phi_3\rangle &= \frac{1}{2}\big(|1111\rangle + |1100\rangle + |0010\rangle + |0001\rangle\big).
\end{aligned} \tag{1.9}$$

[3] In this paper, we will call τ_3 three-tangle and τ_3^2 residual entanglement.

Table 1 $\mathcal{F}_1^{(4)}$, $\mathcal{F}_2^{(4)}$, and $\mathcal{F}_3^{(4)}$ of the maximally entangled and W_4 states

	$\mathcal{F}_1^{(4)}$	$\mathcal{F}_2^{(4)}$	$\mathcal{F}_3^{(4)}$
$\|\Phi_1\rangle$	1	1	$\frac{1}{2}$
$\|\Phi_2\rangle$	$\frac{8}{9}$	0	0
$\|\Phi_3\rangle$	0	0	1
$\|W_4\rangle$	0	0	0

The measures $\mathcal{F}_1^{(4)}$, $\mathcal{F}_2^{(4)}$, and $\mathcal{F}_3^{(4)}$ of $|\Phi_1\rangle$, $|\Phi_2\rangle$, $|\Phi_3\rangle$, and

$$|W_4\rangle = \frac{1}{2}\big(|0111\rangle + |1011\rangle + |1101\rangle + |1110\rangle\big) \tag{1.10}$$

are summarized in Table 1. As Table 1 shows, $|\Phi_1\rangle$ is detected by all measures while $|\Phi_2\rangle$ (or $|\Phi_3\rangle$) is detected by only $\mathcal{F}_1^{(4)}$ (or $\mathcal{F}_3^{(4)}$). As three-qubit system, $|W_4\rangle$ is not detected by all measures.

1.3 Physical motivations

As states earlier, W and GHZ classes represent the true 3-way entanglement in three-qubit system. However, the three-tangle τ_3 and residual entanglement τ_3^2 cannot detect the entanglement of W class, but yield a maximal value to GHZ class. Then, it is natural to ask how much entanglement is detected by τ_3 and τ_3^2 for the rank-2 mixture $\rho(p) = p|\mathrm{GHZ}_3\rangle\langle\mathrm{GHZ}_3| + (1-p)|W_3\rangle\langle W_3|$. This was explored in Ref. [31], whose residual entanglement is

$$\tau_3^2(\rho(p)) = \begin{cases} 0 & \text{for, } 0 \le p \le p_0 \\ g_{\mathrm{I}}(p) & \text{for } p_0 \le p \le p_1 \\ g_{\mathrm{II}}(p) & \text{for } p_1 \le p \le 1 \end{cases} \tag{1.11}$$

where

$$g_{\mathrm{I}}(p) = p^2 - \frac{8\sqrt{6}}{9}\sqrt{p(1-p)^3} \qquad g_{\mathrm{II}}(p) = 1 - (1-p)\left(\frac{3}{2} + \frac{1}{18}\sqrt{465}\right) \tag{1.12}$$

$$p_0 = \frac{4\sqrt[3]{2}}{3 + 4\sqrt[3]{2}} \sim 0.6269 \qquad p_1 = \frac{1}{2} + \frac{3}{310}\sqrt{465} \sim 0.7087.$$

Thus, one can say that the influence of W class is dominant at $0 \le p \le p_0$ while influence of GHZ class is dominant at $p_1 \le p \le 1$. In the intermediate region $p_0 \le p \le p_1$, two classes seem to compete with each other. For three-tangle, similar method can be applied and the result is

Table 2 SLOCC Classification of four-qubit system

SLOCC Classification	Representative states
G_{abcd}	$\|\Phi_1\rangle, \|\Phi_2\rangle, \|\Phi_3\rangle$
L_{ab_3}	$\|W_4\rangle$
L_{abc_2}	$\|0000\rangle$
$L_{a_2b_2}$	$\|0110\rangle + \|0011\rangle$
$L_{a_20_{3\oplus\bar{1}}}$	$\|0011\rangle + \|0101\rangle + \|0110\rangle$
$L_{0_{3\oplus\bar{1}}0_{3\oplus\bar{1}}}$	$\|0000\rangle + \|0111\rangle$
$L_{7\oplus\bar{1}}$	$\|0000\rangle + \|1011\rangle + \|1101\rangle + \|1110\rangle$
L_{a_4}	$\|0001\rangle + \|0110\rangle + \|1000\rangle$
$L_{5\oplus\bar{3}}$	$\|0000\rangle + \|0101\rangle + \|1000\rangle + \|1110\rangle$

$$\tau_3(\rho_p) = \begin{cases} 0 & \text{for } 0 \le p \le p_0 \\ \frac{p-p_0}{1-p_0} & \text{for } p_0 \le p \le 1. \end{cases} \tag{1.13}$$

The expression of τ_3 is much simple than that of τ_3^2. It is mainly due to the fact that τ_3 is a linear invariant under the SLOCC transformation.

One can ask same question to four-qubit system by choosing a rank-2 state. However, situation is much more complicated because the four-qubit system has nine different SLOCC classes [42]. The nine classes and their representative states are summarized in Table 2. Thus, there are too many combinations to choose the rank-2 states. Motivated by the three-qubit case, we choose two classes G_{abcd} and L_{ab_3} and construct the rank-2 state $\rho_j = p|\Phi_j\rangle\langle\Phi_j| + (1-p)|W_4\rangle\langle W_4|$ $(j = 1, 2, 3)$. The purpose of this paper is to compute $\mathcal{F}_j^{(4)}$ and $\mathcal{G}_j^{(4)}$ $(j = 1, 2, 3)$, where $\mathcal{G}_j^{(4)}$ is a linear entanglement monotone defined as

$$\mathcal{G}_1^{(4)} = \left(\mathcal{F}_1^{(4)}\right)^{1/3} \qquad \mathcal{G}_2^{(4)} = \left(\mathcal{F}_2^{(4)}\right)^{1/4} \qquad \mathcal{G}_3^{(4)} = \left(\mathcal{F}_3^{(4)}\right)^{1/6}. \tag{1.14}$$

We will show that as in the three-qubit case, the influence of L_{ab_3} class is strong at $0 \le p \le p_0$, where p_0 is dependent on $|\Phi_j\rangle$ and is larger than the corresponding 3-qubit value 0.6269 for most cases. Of course, with increasing p, the influence of G_{abcd} becomes stronger gradually.

The paper is organized as follows. In Sect. 2, we derive the entanglement of ρ_1, ρ_2, and ρ_3 analytically. We also derive the optimal decompositions explicitly for each range in p. To check the correctness of our results, we use the criterion discussed in Ref. [43], i.e., *entanglement should be a convex hull of the minimum of the characteristic curves*. In Sect. 3, we discuss the possible applications of our results. In the same section, a brief conclusion is given.

2 Entanglement of ρ_j $(j = 1, 2, 3)$

In this section, we will compute the entanglement of $\rho_j = p|\Phi_j\rangle\langle\Phi_j| + (1-p)|W_4\rangle\langle W_4|$. Before explicit calculation, it is convenient to discuss the general method

of our calculation briefly. First, we define a pure state

$$|Z_j(p,\varphi)\rangle = \sqrt{p}|\Phi_j\rangle - e^{i\varphi}\sqrt{1-p}|W_4\rangle. \tag{2.1}$$

Since $|Z_j(p,\varphi)\rangle$ is a pure state, one can compute $\mathcal{F}_i^{(4)}$ $(i=1,2,3)$ of it by making use of Eq. (1.8). As shown below, $\mathcal{F}_i^{(4)}$ has a nontrivial zero at $p=p_0$ for most cases. This is due to the fact that $\mathcal{F}_i^{(4)}$ cannot detect the entanglement of $|W_4\rangle$. Exploiting this fact, we construct the optimal decomposition, which yields $\mathcal{F}_i^{(4)}(\rho_j)=0$ at $0\le p\le p_0$. At $p_0\le p\le 1$ region, we conjecture the optimal decomposition and corresponding $\mathcal{F}_i^{(4)}(\rho_j)$ by making use of the continuity of entanglement with respect to p and convex condition. Same procedure can be applied to the computation of $\mathcal{G}_i^{(4)}(\rho_j)$ $(i,j=1,2,3)$. Finally, we adopt a numerical method, which guarantees the correctness of our guess.

2.1 Case ρ_1

In this subsection, we will compute the entanglement of $\rho_1 = p|\Phi_1\rangle\langle\Phi_1|+(1-p)|W_4\rangle\langle W_4|$.

One can show

$$\begin{aligned}
\mathcal{F}_1^{(4)}[Z_1(p,\varphi)] &= p|p^2-3(1-p)^2e^{4i\varphi}|\\
\mathcal{F}_2^{(4)}[Z_1(p,\varphi)] &= p^2|p^2-4(1-p)^2e^{4i\varphi}|\\
\mathcal{F}_3^{(4)}[Z_1(p,\varphi)] &= \frac{p^6}{2},
\end{aligned} \tag{2.2}$$

where $|Z_1(p,\varphi)\rangle$ is defined in Eq. (2.1) with $j=1$.

1. $\mathcal{F}_1^{(4)}(\rho_1)$ and $\mathcal{G}_1^{(4)}(\rho_1)$

From Eq. (2.2), one can show that $\mathcal{F}_1^{(4)}[Z_1(p,\varphi)]$ has a nontrivial zero $(\varphi=0)$

$$p_0 = \frac{\sqrt{3}}{\sqrt{3}+1} \approx 0.634. \tag{2.3}$$

The existence of finite p_0 guarantees that $\mathcal{F}_1^{(4)}(\rho_1)$ should vanish at $0\le p\le p_0$. At $p=p_0$, this fact can be verified because we have the optimal decomposition

$$\begin{aligned}
\rho_1(p_0) = \frac{1}{4}\Bigg[&|Z_1(p_0,0)\rangle\langle Z_1(p_0,0)|+|Z_1\left(p_0,\frac{\pi}{2}\right)\rangle\langle Z_1\left(p_0,\frac{\pi}{2}\right)|\\
&+|Z_1(p_0,\pi)\rangle\langle Z_1(p_0,\pi)|+|Z_1\left(p_0,\frac{3\pi}{2}\right)\rangle\langle Z_1\left(p_0,\frac{3\pi}{2}\right)|\Bigg].
\end{aligned} \tag{2.4}$$

At the region $0\le p<p_0$, $\mathcal{F}_1^{(4)}(\rho_1)$ should vanish too because one can find the following optimal decomposition

$$\rho_1(p) = \frac{p}{p_0}\rho_1(p_0) + \left(1 - \frac{p}{p_0}\right)|W_4\rangle\langle W_4|. \tag{2.5}$$

Combining these facts, one can conclude that $\mathcal{F}_1^{(4)}(\rho_1) = 0$ at $0 \le p \le p_0$.

Next, we consider the $p_0 \le p \le 1$ region. Eq. (2.4) at $p = p_0$ strongly suggests that the optimal decomposition at this region is

$$\begin{aligned}\rho_1(p) = \frac{1}{4}\Bigg[&|Z_1(p,0)\rangle\langle Z_1(p,0)| + |Z_1\left(p,\frac{\pi}{2}\right)\rangle\langle Z_1\left(p,\frac{\pi}{2}\right)| \\ &+ |Z_1(p,\pi)\rangle\langle Z_1(p,\pi)| + |Z_1\left(p,\frac{3\pi}{2}\right)\rangle\langle Z_1\left(p,\frac{3\pi}{2}\right)|\Bigg].\end{aligned} \tag{2.6}$$

If Eq. (2.6) is a correct optimal decomposition in this region, $\mathcal{F}_1^{(4)}(\rho_1)$ reduces to

$$\mathcal{F}_1^{(4)}(\rho_1) = p(6p - 2p^2 - 3). \tag{2.7}$$

Since the right-hand side of Eq. (2.7) is convex, our conjecture [Eq. (2.6)] seems to be right. In conclusion, we can write

$$\mathcal{F}_1^{(4)}(\rho_1) = \theta(p - p_0)p(6p - 2p^2 - 3), \tag{2.8}$$

where $\theta(x)$ is a step function defined as

$$\theta(x) = \begin{cases} 1 & x \ge 0 \\ 0 & x < 0. \end{cases} \tag{2.9}$$

However, if our choice Eq. (2.6) is incorrect, Eq. (2.8) is merely an upper bound of $\mathcal{F}_1^{(4)}(\rho_1)$. Thus, we need to prove that Eq. (2.8) is really optimal value. To prove this, we should examine, in principle, all possible decompositions of ρ_1, i.e., $\rho_1 = \sum_i p_i|\psi_i\rangle\langle\psi_i|$, and minimize the corresponding value $\sum_i p_i\mathcal{F}_1^{(4)}(\psi_i)$. However, it is impossible because ρ_1 has infinite number of decomposition.

In order to escape this difficulty to some extent, one may rely on Caratheodory's theorem for convex hull [44], which states that for four-qubit rank-2 states, five vector decomposition is sufficient to minimize $\mathcal{F}_1^{(4)}(\rho_1)$. Thus, we need to investigate decompositions with 2, 3, 4, or 5 vectors. This method was used in Ref. [31] to minimize the residual entanglement of three-qubit rank-2 mixture. Still, however, it is difficult, at least for us, to parameterize all decompositions with first few vectors.

In this paper, therefore, we will adopt the alternative numerical method presented in Ref. [43]. We plot the p-dependence of $\mathcal{F}_1^{(4)}[Z_1(p,\varphi)]$ for various φ (See solid lines of Fig. 1a). These curves have been referred as the characteristic curves. As Ref. [43] showed, $\mathcal{F}_1^{(4)}(\rho_1)$ is a convex hull of the minimum of the characteristic curves. Fig. 1a indicates that Eq.(2.8) (thick dashed line) is really the convex characteristic curve, which implies that Eq.(2.8) is really optimal. This method was also used in Ref. [33] to minimize the residual entanglement of three-qubit rank-3 mixture.

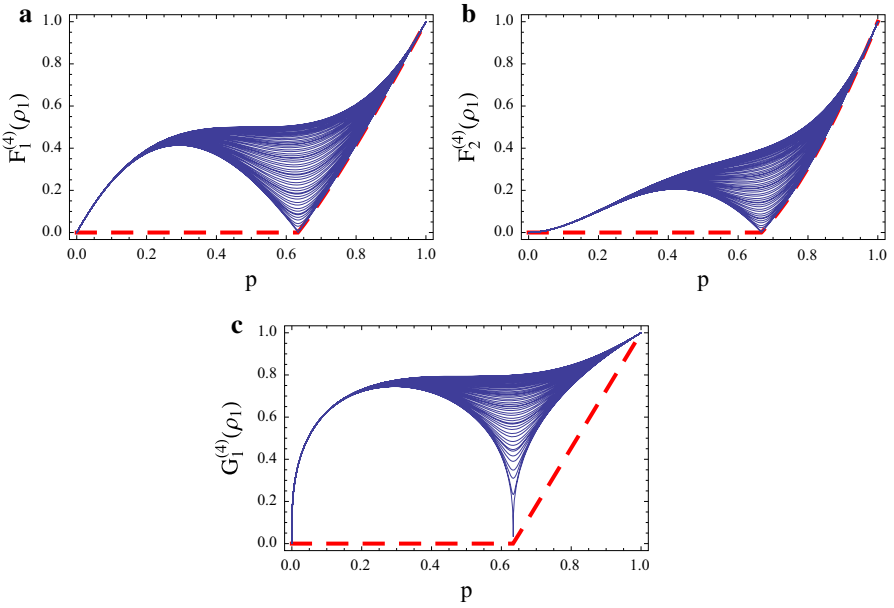

Fig. 1 (Color online) Plot of the p dependence of **a** $\mathcal{F}_1^{(4)}[Z_1(p,\varphi)]$, **b** $\mathcal{F}_2^{(4)}[Z_1(p,\varphi)]$, and **c** $\mathcal{G}_1^{(4)}[Z_1(p,\varphi)]$ in Eq. (2.2). We have chosen φ from 0 to 2π as an interval 0.1. The *thick dashed lines* correspond to $\mathcal{F}_1^{(4)}(\rho_1)$ in Eq. (2.8), $\mathcal{F}_2^{(4)}(\rho_1)$ in Eq. (2.13) and $\mathcal{G}_1^{(4)}(\rho_1)$ in Eq. (2.11). These figures indicate that Eqs. (2.8), (2.13), and (2.11) are convex hull of the minimum of the characteristic curves

Now, let us consider $\mathcal{G}_1^{(4)}(\rho_1)$. It is easy to show that $\mathcal{G}_1^{(4)}(\rho_1)$ vanishes at $0 \leq p \leq p_0$ due to the optimal decomposition Eq. (2.5). If one chooses Eq. (2.6) as an optimal decomposition at $p_0 \leq p \leq 1$, the resulting $\mathcal{G}_1^{(4)}(\rho_1)$ is not convex in the full range. Thus, we should adopt a technique introduced in Ref. [31–35]. In this case, the optimal decomposition is

$$\rho_1(p) = \frac{p-p_0}{1-p_0}|\Phi_1\rangle\langle\Phi_1| + \frac{1-p}{1-p_0}\rho_1(p_0), \tag{2.10}$$

which results in $\mathcal{G}_1^{(4)}(\rho_1) = (p-p_0)/(1-p_0)$. Combining all these facts, one can conclude

$$\mathcal{G}_1^{(4)}(\rho_1) = \theta(p-p_0)\frac{p-p_0}{1-p_0}. \tag{2.11}$$

To confirm that Eq. (2.11) is correct, we plot the characteristic curves $\mathcal{G}_1^{(4)}[Z_1(p,\varphi)]$ for various φ as solid lines and Eq. (2.11) as thick dashed line in Fig. 1c. This figure shows that Eq. (2.11) is convex hull of the minimum of the characteristic curves, which strongly supports the validity of Eq. (2.11).

2.$\mathcal{F}_2^{(4)}(\rho_1)$ and $\mathcal{G}_2^{(4)}(\rho_1)$

Table 3 Summary of $\mathcal{F}_j^{(4)}$ and $\mathcal{G}_j^{(4)}$ for ρ_1

j	$\mathcal{F}_j^{(4)}$	$\mathcal{G}_j^{(4)}$	p_0
$j=1$	$p(6p-2p^2-3)\theta(p-p_0)$	$\frac{p-p_0}{1-p_0}\theta(p-p_0)$	$\frac{\sqrt{3}}{\sqrt{3}+1}\approx 0.634$
$j=2$	$p^2[p^2-4(1-p)^2]\theta(p-p_0)$	$\frac{p-p_0}{1-p_0}\theta(p-p_0)$	$\frac{2}{3}\approx 0.667$
$j=3$	$\frac{p^6}{2}$	$\frac{p}{2^{1/6}}$	

From Eq. (2.2), one can notice that $\mathcal{F}_2^{(4)}[Z_1(p,\varphi)]$ has a nontrivial zero ($\varphi=0$)

$$p_0=\frac{2}{3}\approx 0.667. \tag{2.12}$$

Thus, Eq. (2.5) and Eq. (2.6) with $p_0=2/3$ can be the optimal decompositions for $\mathcal{F}_2^{(4)}(\rho_1)$ at $0\le p\le p_0$ and $p_0\le p\le 1$, respectively. Then, the resulting $\mathcal{F}_2^{(4)}(\rho_1)$ becomes

$$\mathcal{F}_2^{(4)}(\rho_1)=\theta(p-p_0)p^2[p^2-4(1-p)^2]. \tag{2.13}$$

In order to confirm that our result (2.13) is correct, we plot the characteristic curves for various φ (solid lines) and Eq. (2.13) (thick dashed line) in Fig. 1b. As Fig. 1b exhibits, our result (2.13) is convex hull of the minimum of the characteristic curves, which strongly supports that Eq. (2.13) is really optimal one.

Similarly, $\mathcal{G}_2^{(4)}(\rho_1)$ becomes Eq. (2.11) with changing only p_0 to $2/3$. The corresponding optimal decompositions are Eq. (2.5) at $0\le p\le p_0$ and Eq. (2.10) at $p_0\le p\le 1$, respectively. Of course, we have to change p_0 to $2/3$.

3.$\mathcal{F}_3^{(4)}(\rho_1)$ and $\mathcal{G}_3^{(4)}(\rho_1)$

Eq. (2.2) shows that $\mathcal{F}_3^{(4)}[Z_1(p,\varphi)]$ does not have nontrivial zero. In addition, it is independent of the phase angle φ. This fact may indicate that there are infinite number of optimal decompositions for $\mathcal{F}_3^{(4)}(\rho_1)$. The simplest one is

$$\rho_1(p)=\frac{1}{2}|Z_1(p,0)\rangle\langle Z_1(p,0)|+\frac{1}{2}|Z_1(p,\pi)\rangle\langle Z_1(p,\pi)|, \tag{2.14}$$

which gives $\mathcal{F}_3^{(4)}(\rho_1)=p^6/2$. If one chooses Eq. (2.14) as an optimal decomposition for $\mathcal{G}_3^{(4)}(\rho_1)$, it generates $\mathcal{G}_3^{(4)}(\rho_1)=p/2^{1/6}$. Since it is not concave, we do not need to adopt a technique to make $\mathcal{G}_3^{(4)}(\rho_1)$ convex as we did previously. We summarize our results in Table 3.

2.2 Case ρ_2

In this subsection, we would like to quantify the entanglement of ρ_2. Above all, we should say that Table 1 implies

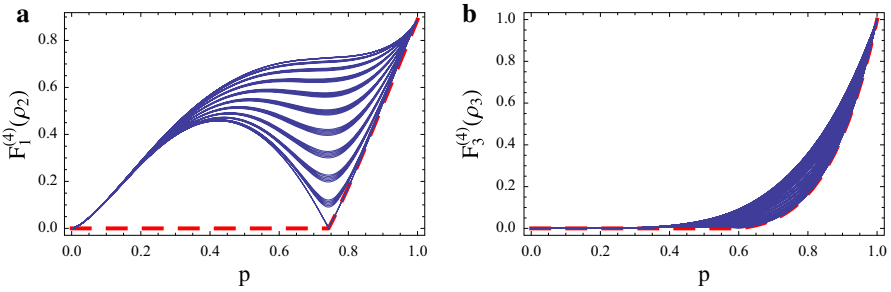

Fig. 2 (Color online) Plot of the p dependence of **a** $\mathcal{F}_1^{(4)}[Z_2(p,\varphi)]$ in Eq. (2.16) and **b** $\mathcal{F}_3^{(4)}[Z_3(p,\varphi)]$ in Eq. (2.29). We have chosen φ from 0 to 2π as an interval 0.1. The *thick dashed lines* correspond to $\mathcal{F}_1^{(4)}(\rho_2)$ in Eq. (2.25) and $\mathcal{F}_3^{(4)}(\rho_3)$ in Eq. (2.34). These figures indicate that Eqs. (2.25), (2.34) are convex hull of the minimum of the characteristic curves

$$\mathcal{F}_2^{(4)}(\rho_2) = \mathcal{G}_2^{(4)}(\rho_2) = \mathcal{F}_3^{(4)}(\rho_2) = \mathcal{G}_3^{(4)}(\rho_2) = 0, \tag{2.15}$$

because $\rho_2 = p|\Phi_2\rangle\langle\Phi_2| + (1-p)|W_4\rangle\langle W_4|$ itself is an optimal decomposition for those entanglement measures. This fact is due to the fact that $\mathcal{F}_2^{(4)}$ and $\mathcal{F}_3^{(4)}$ cannot detect both $|\Phi_2\rangle$ and $|W_4\rangle$.

Let us now compute $\mathcal{F}_1^{(4)}(\rho_2)$ and $\mathcal{G}_1^{(4)}(\rho_2)$. It is straightforward to show

$$\mathcal{F}_1^{(4)}[Z_2(p,\varphi)] = \frac{8}{9}p^{3/2}|p^{3/2} - 2\sqrt{6}(1-p)^{3/2}e^{3i\varphi}|, \tag{2.16}$$

where $|Z_2(p,\varphi)\rangle$ is given in Eq. (2.1). We notice that $\mathcal{F}_1^{(4)}[Z_2(p,\varphi)]$ has a nontrivial zero ($\varphi = 0$)

$$p_0 = \frac{(2\sqrt{6})^{2/3}}{1 + (2\sqrt{6})^{2/3}} \approx 0.743. \tag{2.17}$$

Thus, $\mathcal{F}_1^{(4)}(\rho_2)$ vanishes at $0 \le p \le p_0$ because one can find the optimal decomposition

$$\rho_2(p) = \frac{p}{p_0}\rho_2(p_0) + \left(1 - \frac{p}{p_0}\right)|W_4\rangle\langle W_4|, \tag{2.18}$$

where

$$\rho_2(p_0) = \frac{1}{3}\left[|Z_2(p_0,0)\rangle\langle Z_2(p_0,0)| + |Z_2\left(p_0, \frac{2\pi}{3}\right)\rangle\langle Z_2\left(p_0, \frac{2\pi}{3}\right)| + |Z_2\left(p_0, \frac{4\pi}{3}\right)\rangle\langle Z_2\left(p_0, \frac{4\pi}{3}\right)|\right]. \tag{2.19}$$

As the previous cases, we adopt, as a trial, the optimal decomposition at $p_0 \le p \le 1$ as

$$\rho_2(p) = \frac{1}{3}\left[|Z_2\,(p,0)\rangle\langle Z_2\,(p,0)\,| + |Z_2\left(p,\frac{2\pi}{3}\right)\rangle\langle Z_2\left(p,\frac{2\pi}{3}\right)| + |Z_2\left(p,\frac{4\pi}{3}\right)\rangle\langle Z_2\left(p,\frac{4\pi}{3}\right)|\right]. \tag{2.20}$$

Then $\mathcal{F}_1^{(4)}(\rho_2)$ becomes $g_{\rm I}(p)$, where

$$g_{\rm I}(p) = \frac{8}{9}p^{3/2}\left[p^{3/2} - 2\sqrt{6}(1-p)^{3/2}\right]. \tag{2.21}$$

However, $g_{\rm I}(p)$ is not convex at the region $p \geq p_* \approx 0.9196$. Thus, we should adopt the technique previously used again to make $g_{\rm I}(p)$ convex at the large-p region.

Now, we define p_1 such as $p_0 \leq p_1 \leq p_*$. The parameter p_1 will be determined later. At the region $p_1 \leq p \leq 1$, we adopt the optimal decomposition for $\mathcal{F}_1^{(4)}(\rho_2)$ as a following form:

$$\rho_2(p) = \frac{p-p_1}{1-p_1}|\Phi_2\rangle\langle\Phi_2| + \frac{1-p}{1-p_1}\rho_2(p_1), \tag{2.22}$$

where

$$\rho_2(p_1) = \frac{1}{3}\left[|Z_2\,(p_1,0)\rangle\langle Z_2\,(p_1,0)\,| + |Z_2\left(p_1,\frac{2\pi}{3}\right)\rangle\langle Z_2\left(p_1,\frac{2\pi}{3}\right)| + |Z_2\left(p_1,\frac{4\pi}{3}\right)\rangle\langle Z_2\left(p_1,\frac{4\pi}{3}\right)|\right]. \tag{2.23}$$

Equation (2.22) leads $\mathcal{F}_1^{(4)}(\rho_2)$ to $g_{\rm II}(p)$ at the large-p region, where

$$g_{\rm II}(p) = \frac{8}{9}\left[\frac{p-p_1}{1-p_1} + \frac{1-p}{1-p_1}\left\{p_1^3 - 2\sqrt{6}p_1^{3/2}(1-p_1)^{3/2}\right\}\right]. \tag{2.24}$$

As expected, $g_{\rm II}(p)$ is convex at $p_1 \leq p \leq 1$. The parameter p_1 is determined by $\frac{\partial g_{\rm II}}{\partial p_1} = 0$, which yields $p_1 \approx 0.861$[4]. Thus, $\mathcal{F}_1^{(4)}(\rho_2)$ can be summarized as

$$\mathcal{F}_1^{(4)}(\rho_2) = \begin{cases} 0 & 0 \leq p \leq p_0 \\ g_{\rm I}(p) & p_0 \leq p \leq p_1 \\ g_{\rm II}(p) & p_1 \leq p \leq 1. \end{cases} \tag{2.25}$$

In order to confirm again that Eq. (2.25) is correct, we plot the p-dependence of the characteristic curves (solid lines) in Fig. 2a for various φ. Our result (2.25) is plotted as a thick dashed line. This figure shows that our result (2.25) is a convex characteristic curve, which strongly supports that our result (2.25) is correct.

[4] The parameter p_1 is obtained by an equation $6p_1(4p_1-3)^2 = (1-p_1)(1+2p_1)^2$.

Now, let us compute $\mathcal{G}_1^{(4)}(\rho_2)$. At $0 \le p \le p_0$, $\mathcal{G}_1^{(4)}(\rho_2)$ should be zero due to Eq. (2.18). If we adopt Eq. (2.20) as an optimal decomposition, $\mathcal{G}_1^{(4)}(\rho_2) = g_1^{1/3}(p)$ is obtained. However, it is not convex in the full range. Therefore, we have to choose

$$\rho_2(p) = \frac{p - p_0}{1 - p_0}|\Phi_2\rangle\langle\Phi_2| + \frac{1 - p}{1 - p_0}\rho_2(p_0) \tag{2.26}$$

as an optimal decomposition, which results in

$$\mathcal{G}_1^{(4)}(\rho_2) = \theta(p - p_0)\left(\frac{8}{9}\right)^{1/3}\frac{p - p_0}{1 - p_0}. \tag{2.27}$$

2.3 Case ρ_3

In this subsection, we will compute the entanglement of $\rho_3 = p|\Phi_3\rangle\langle\Phi_3| + (1 - p)|W_4\rangle\langle W_4|$. Since $\mathcal{F}_1^{(4)}$ and $\mathcal{F}_2^{(4)}$ cannot detect both $|\Phi_3\rangle$ and $|W_4\rangle$, it is easy to show

$$\mathcal{F}_1^{(4)}(\rho_3) = \mathcal{G}_1^{(4)}(\rho_3) = \mathcal{F}_2^{(4)}(\rho_3) = \mathcal{G}_2^{(4)}(\rho_3) = 0. \tag{2.28}$$

Now, let us compute $\mathcal{F}_3^{(4)}(\rho_3)$ and $\mathcal{G}_3^{(4)}(\rho_3)$. For $|Z_3(p, \varphi)\rangle$ in Eq. (2.1), it is possible to show that $\mathcal{F}_3^{(4)}[Z_3(p, \varphi)]$ reduces to

$$\mathcal{F}_3^{(4)}[Z_3(p, \varphi)] = p^5\left|p - \frac{3}{2}(1 - p)e^{2i\varphi}\right|. \tag{2.29}$$

Equation. (2.29) implies that $\mathcal{F}_3^{(4)}[Z_3(p, \varphi)]$ has a nontrivial zero ($\varphi = 0$)

$$p_0 = \frac{3}{5} = 0.6. \tag{2.30}$$

Thus, $\mathcal{F}_3^{(4)}(\rho_3)$ should be zero at the region $0 \le p \le p_0$, and its optimal decomposition is

$$\rho_3(p) = \frac{p}{p_0}\rho_3(p_0) + \left(1 - \frac{p}{p_0}\right)|W_4\rangle\langle W_4|, \tag{2.31}$$

where

$$\rho_3(p_0) = \frac{1}{2}\left[|Z_3(p_0, 0)\rangle\langle Z_3(p_0, 0)| + |Z_3(p_0, \pi)\rangle\langle Z_3(p_0, \pi)|\right]. \tag{2.32}$$

If we adopt the optimal decomposition at $p_0 \le p \le 1$ as a form

$$\rho_3(p) = \frac{1}{2}\left[|Z_3(p, 0)\rangle\langle Z_3(p, 0)| + |Z_3(p, \pi)\rangle\langle Z_3(p, \pi)|\right], \tag{2.33}$$

the resulting $\mathcal{F}_3^{(4)}(\rho_3)$ becomes $\frac{5}{2}p^5\left(p-\frac{3}{5}\right)$. Since this is convex, we conclude

$$\mathcal{F}_3^{(4)}(\rho_3) = \theta(p-p_0)\frac{5}{2}p^5\left(p-\frac{3}{5}\right). \tag{2.34}$$

In order to prove that Eq. (2.34) is correct, we plot again the characteristic curves (solid lines) and our result (2.34) (thick dashed line) in Fig. 2b, which supports that Eq. (2.34) is optimal one.

Finally, let us compute $\mathcal{G}_3^{(4)}(\rho_3)$. If we take Eq. (2.33) as an optimal decomposition for $\mathcal{G}_3^{(4)}(\rho_3)$ at $p_0 \le p \le 1$, the result is not convex in the full range of this region. Thus, we should choose

$$\rho_3(p) = \frac{p-p_0}{1-p_0}|\Phi_3\rangle\langle\Phi_3| + \frac{1-p}{1-p_0}\rho_3(p_0) \tag{2.35}$$

as an optimal decomposition, which simply results in the right-hand side of Eq. (2.11) with $p_0 = 3/5$.

3 Discussion and conclusions

We compute the three kinds of true four-way entanglement measures $\mathcal{F}_j^{(4)}$ $(j = 1, 2, 3)$ and their corresponding linear entanglement monotones $\mathcal{G}_j^{(4)}$ $(j = 1, 2, 3)$ analytically for four-qubit rank-2 mixed states $\rho_j = p|\Phi_j\rangle\langle\Phi_j| + (1-p)|W_4\rangle\langle W_4|$ $(j = 1, 2, 3)$. All optimal decompositions consist of 2, 3, 4, and 5 vectors.

Our results can be used to find many different mixed states, which have vanishing entanglement. For example, let us consider $\mathcal{F}_1^{(4)}$ with p_0 in Eq. (2.17). Let us represent, for simplicity, $|\Phi_2\rangle$ and $|W_4\rangle$ as

$$|\Phi_2\rangle = \begin{pmatrix}1\\0\end{pmatrix} \quad |W_4\rangle = \begin{pmatrix}0\\1\end{pmatrix}. \tag{3.1}$$

Imagine the two-dimensional space spanned by $|\Phi_2\rangle$ and $|W_4\rangle$ represented by a Bloch sphere. Then, the states in the Bloch sphere can be expressed as $\rho = \frac{1}{2}(\mathbb{1} + \boldsymbol{r}\cdot\boldsymbol{\sigma})$, where $|\boldsymbol{r}| = 1$ and $|\boldsymbol{r}| < 1$ denote the pure and mixed states, respectively. In this representation, the Bloch vectors of $|\Phi_2\rangle$, $|W_4\rangle$, and $|Z_2(p_0,\varphi)\rangle$ are

$$\begin{aligned}&\boldsymbol{r}(\Phi_2) = (0,0,1) \qquad \boldsymbol{r}(W_4) = (0,0,-1)\\ &\boldsymbol{r}(Z_2(p_0,\varphi)) = (-2\sqrt{p_0(1-p_0)}\cos\varphi, -2\sqrt{p_0(1-p_0)}\sin\varphi, 2p_0-1).\end{aligned} \tag{3.2}$$

Thus, any states located in the tetrahedron , whose vertices are $(0,0,-1)$, $(-2\sqrt{p_0(1-p_0)}, 0, 2p_0-1)$, $(\sqrt{p_0(1-p_0)}, -\sqrt{3p_0(1-p_0)}, 2p_0-1)$, and $(\sqrt{p_0(1-p_0)}, \sqrt{3p_0(1-p_0)}, 2p_0-1)$ in the Bloch sphere representation, have vanishing $\mathcal{F}_1^{(4)}$ and $\mathcal{G}_1^{(4)}$.

One can use our results to discuss the monogamy properties [45] of entanglement. For this purpose, however, we should compute the entanglement for the sub-states of

Table 4 Entanglement for sub-states of $\rho_j \quad (j = 1, 2, 3)$

	$\mathcal{C}$ (concurrence)	τ (three-tangle)
ρ_1	$\frac{1}{2}\left(1-2\sqrt{p}-p\right)\theta(\alpha_1-p) \quad \left(\alpha_1=(\sqrt{2}-1)^2\right)$	0
ρ_2	$\left(\frac{3-p}{6}-\frac{\sqrt{2}}{3}\sqrt{p(3-p)}\right)\theta(\alpha_2-p) \quad \left(\alpha_2=\frac{1}{3}\right)$	?
	$\mathcal{C}_{AB}=\frac{1}{2}\left(1-2\sqrt{p}-p\right)\theta(\alpha_1-p)$	
ρ_3	$\mathcal{C}_{AC}=\mathcal{C}_{AD}=\mathcal{C}_{BC}=\mathcal{C}_{BD}$	$\tau_{ACD}=\tau_{BCD}=0$
	$=\frac{1}{2}\left(1-p-\sqrt{p(2-p)}\right)\theta(\alpha_3-p) \quad \left(\alpha_3=\frac{2-\sqrt{2}}{2}\right)$	$\tau_{ABC}=\tau_{ABD}=?$
	$\mathcal{C}_{CD}=\frac{1}{2}\left\{1-\sqrt{\frac{p}{2}}\left(\sqrt{1+\sqrt{p(2-p)}}+\sqrt{1-\sqrt{p(2-p)}}\right)\right\}$	

$\rho_j \quad (j = 1, 2, 3)$. The entanglement of the sub-states is summarized in Table 4. As this table shows, some three-tangle, at least for us, cannot be computed analytically. This is because still we do not have a closed formula for computing the three-tangles.

As mentioned above, there are nine SLOCC classes in the four-qubit system. Therefore, many rank-2 states can be constructed by choosing different classes. If, for example, G_{abcd} and $L_{7_{\oplus\bar{1}}}$ are chosen, one can construct the rank-2 state

$$\pi_j = p|\Phi_j\rangle\langle\Phi_j| + (1-p)|\xi\rangle\langle\xi|, \tag{3.3}$$

where $|\xi\rangle = (|0000\rangle + |1011\rangle + |1101\rangle + |1110\rangle)/2$. Probably, our calculation procedure enables us to compute the entanglement of π_2 and π_3 although we have not checked it explicitly. For π_1, however, our procedure does not seem to work because of $\langle\xi|\Phi_1\rangle \neq 0$. Using Table 2, one can construct many higher rank states. If, for example, G_{abcd}, $L_{7_{\oplus\bar{1}}}$, and L_{a_4} are chosen, one can construct the rank-3 state such as

$$\sigma_j = p|\Phi_j\rangle\langle\Phi_j| + q|\xi\rangle\langle\xi| + (1-p-q)|\eta\rangle\langle\eta|, \tag{3.4}$$

where $|\eta\rangle = (|0001\rangle + |0110\rangle + |1000\rangle)/\sqrt{3}$. However, it seems to be highly difficult to compute the entanglement of higher rank states.

The most remarkable achievement and novelty of this paper is deriving the entanglement of four-qubit mixed states using an analytical approach. Thus, our result may serve as a quantitative reference for future studies of entanglement in quadripartite and/or multipartite mixed states.

Acknowledgments This research was supported by the Basic Science Research Program through the National Research Foundation of Korea(NRF) funded by the Ministry of Education, Science and Technology(2011-0011971).

References

1. Nielsen, M.A., Chuang, I.L.: Quantum computation and quantum information. Cambridge University Press, Cambridge, (2000)

2. Horodecki, R., Horodecki, P., Horodecki, M., Horodecki, K.: Quantum entanglement. Rev. Mod. Phys. **81**, 865 (2009). quant-ph/0702225 and references therein
3. Bennett, C.H., Brassard, G., Crepeau, C., Jozsa, R., Peres, A., Wootters, W.K.: Teleporting an unknown quantum state via dual classical and Einstein–Podolsky–Rosen channles. Phys. Rev. Lett. **70**, 1895 (1993)
4. Bennett, C.H., Wiesner, S.J.: Communication via one- and two-particle operators on Einstein–Podolsky–Rosen states. Phys. Rev. Lett. **69**, 2881 (1992)
5. Scarani, V., Lblisdir, S., Gisin, N., Acin, A.: Quantum cloning. Rev. Mod. Phys. **77**, 1225 (2005). quant-ph/0511088 and references therein
6. Ekert, A.K.: Quantum cryptography based on bells theorem. Phys. Rev. Lett. **67**, 661 (1991)
7. Kollmitzer, C., Pivk, M.: Applied Quantum Cryptography. Springer, Heidelberg, (2010)
8. Ladd, T.D., Jelezko, F., Laflamme, R., Nakamura, Y., Monroe, C., O'Brien, J.L.: Quantum computers. Nature **464**, 45 (2010). arXiv:1009.2267 (quant-ph)
9. Vidal, G.: Efficient classical simulation of slightly entangled quantum computations. Phys. Rev. Lett. **91**, 147902 (2003). quant-ph/0301063
10. Bennett, C.H., DiVincenzo, D.P., Smokin, J.A., Wootters, W.K.: Mixed-state entanglement and quantum error correction. Phys. Rev. A **54**, 3824 (1996). quant-ph/9604024
11. Vedral, V., Plenio, M.B., Rippin, M.A., Knight, P.L.: Quantifying entanglement. Phys. Rev. Lett. **78**, 2275 (1997). quant-ph/9702027
12. Vedral, V., Plenio, M.B.: Entanglement measures and purification procedures. Phys. Rev. **57**, 1619 (1998). quant-ph/9707035
13. Smolin, J.A.: Four-party unlockable bound entangled state. Phys. Rev. A. **63**, 032306 (2001). quant-ph/0001001
14. Ghosh, S., Kar, G., Roy, A., Sen(De), A., Sen, U.: Distinguishability of bell states. Phys. Rev. Lett. **87**, 277902 (2001). quant-ph/0106148
15. Chen, Y.X., Jin, J.S., Yang, D.: Distillation of multiple copies of bell states. Phys. Rev. A. **67**, 014302 (2003)
16. Yang, D., Chen, Y.X.: Mixture of multiple copies of maximally entangled states is quasipure. Phys. Rev. A **69**, 024302 (2004)
17. Miranowicz, A., Ishizaka, S.: Closed formula for the relative entropy of entanglement. Phys. Rev. A **78**, 032310 (2008). arXiv:0805.3134 (quant-ph)
18. Kim, H., Hwang, M.R., Jung, E., Park, D.K.: Difficulties in analytic computation for relative entropy of entanglement. ibid. A **81**, 052325 (2010). arXiv:1002.4695 (quant-ph)
19. Park, D.K.: Relative entropy of entanglement for two-qubit state with z-directional Bloch vectors. Int. J. Quantum. Inf. **8**, 869 (2010). arXiv:1005.4777 (quant-ph)
20. Friedland, S., Gour, G.: Closed formula for the relative entropy of entanglement in all dimensions. J. Math. Phys. **52**, 052201 (2011). arXiv:1007.4544 (quant-ph)
21. M. W. Girard, G. Gour, and S. Friedland, On convex optimization problems in quantum information theory.arXiv:1402.0034 (quant-ph)
22. Jung, E., Park, D.K.: REE From EOF. Quantum. Inf. Process. **14**, 531 (2015). arXiv:1404.7708 (quant-ph)
23. Uhlmann, A.: Fidelity and concurrence of conjugate states. Phys. Rev. **62**, 032307 (2000). quant-ph/9909060
24. Hill, S., Wootters, W.K.: Entanglement of a pair of quantum bits. Phys. Rev. Lett. **78**, 5022 (1997). quant-ph/9703041
25. W. K. Wootters, Entanglement of formation of an arbitrary state of two qubits. ibid. **80** 2245 (1998) quant-ph/9709029
26. Bennett, C.H., Popescu, S., Rohrlich, D., Smolin, J.A., Thapliyal, A.V.: Exact and asymptotic measures of multipartite pure-state entanglement. Phys. Rev. **63**, 012307 (2000). quant-ph/9908073
27. Dür, W., Vidal, G., Cirac, J.I.: Three qubits can be entangled in two inequivalent ways. Phys. Rev. A **62**, 062314 (2000). quant-ph/0005115
28. Acín, A., Bruß, D., Lewenstein, M., Sanpera, A.: Classification of mixed three-qubit states. Phys. Rev. Lett. **87**, 040401 (2001). quant-ph/0103025
29. Verstraete, F., Dehaene, J., De Moor, D.: Normal forms and entanglement measures for multipartite quantum states. Phys. Rev. A **68**, 012103 (2003). quant-ph/0105090
30. Coffman, V., Kundu, J., Wootters, W.K.: Distributed entanglement. Phys. Rev. A **61**, 052306 (2000). quant-ph/9907047

31. Lohmayer, R., Osterloh, A., Siewert, j, Uhlmann, A.: Entangled three-qubit states without concurrence and three-tangle. Phys. Rev. Lett. **97**, 260502 (2006). quant-ph/0606071
32. Eltschka, C., Osterloh, A., Siewert, J., Uhlmann, A.: Three-tangle for mixtures of generalized GHZ and generalized W states. New J. Phys. **10**, 043014 (2008). arXiv:0711.4477 (quant-ph)
33. Jung, E., Hwang, M.R., Park, D.K., Son, J.W.: Three-tangle for rank-3 mixed states: mixture of Greenberger–Horne–Zeilinger, W and flipped W states. Phys. Rev. A **79**, 024306 (2009). arXiv:0810.5403 (quant-ph)
34. Jung, E., Park, D.K., Son, J.W.: Three-tangle does not properly quantify tripartite entanglement for Greenberger–Horne–Zeilinger-type state. Phys. Rev. A **80**, 010301(R) (2009). arXiv:0901.2620 (quant-ph)
35. Jung, E., Hwang, M.R., Park, D.K., Tamaryan, S.: Three-party entanglement in tripartite teleportation scheme through noisy channels. Quantum Inf. Comput. **10**, 0377 (2010). arXiv:0904.2807 (quant-ph)
36. Eltschka, C., Siewert, J.: Entanglement of three-qubit Greenberger–Horne–Zeilinger-symmetric states. Phys. Rev. Lett. **108**, 020502 (2012). arXiv:1304.6095 (quant-ph)
37. Siewert, J., Eltschka, C.: Quantifying tripartite entanglement of three-qubit generalized werner states. Phys. Rev. Lett. **108**, 230502 (2012)
38. Osterloh, A., Siewert, J.: Constructing N-qubit entanglement monotones from antilinear operators. Phys. Rev. A **72**, 012337 (2005). quant-ph/0410102
39. Doković, D.Ž., Osterloh, A.: On polynomial invariants of several qubits. J. Math. Phys. **50**, 033509 (2009). arXiv:0804.1661 (quant-ph)
40. Osterloh, A., Siewert, J.: The invariant-comb approach and its relation to the balancedness of multiple entangled states. New J. Phys. **12**, 075025 (2010). arXiv:0908.3818 (quant-ph)
41. Osterloh, A., Siewert, J.: Entanglement monotones and maximally entangled states in multipartite qubit systems. Inf. Comput. **4**, 0531 (2006). quant-ph/0506073
42. Verstraete, F., Dehaene, J., De Moor, B., Verschelde, H.: Four qubits can be entangled in nine different ways. Phys. Rev. A **65**, 052112 (2002)
43. Osterloh, A., Siewert, J., Uhlmann, A.: Tangles of superpositions and the convex-roof extension. Phys. Rev. A **77**, 032310 (2008). arXiv:0710.5909 (quant-ph)
44. Hiriart-Urruty, J.-B., Lemaréchal, C.L.: Convex Analysis and Minimization Algorithms. Springer, Berlin, (1996)
45. C. Eltschka and J. Siewert, Monogamy equalities for qubit entanglement from Lorentz invariance.arXiv:1407.8195 (quant-ph)